On the Kinetics of Ice Crystallization in Batch Crystallizers

The population balance equation with respect to ice crystal size in a batch crystallizer was solved, taking into account the crystal size dependency of growth rate, and the temperature change with crystal growth was calculated. Both the temperature change and the crystal size distribution obtained theoretically were in fairly good agreement with the experimental factors measured in pure water and in a 5% dextran solution.

YOSHIHITO SHIRAI, KAZUHIRO NAKANISHI, RYUICHI MATSUNO and TADASHI KAMIKUBO

Department of Food Science and Technology
Faculty of Agriculture
Kyoto University
Sakyo-ku, Kyoto 606 Japan

SCOPE

Although freeze concentration is considered to be a very desirable method for the concentration of liquid foods for quality preservation, its development has been hampered by the fact that recovery of the concentrated solute remaining on the ice crystal surface is difficult due to formation of very fine ice particles. Thus a method for obtaining precise information on the kinetics of ice crystallization in liquid foods should be established.

With a steady state method using a continuous crystallizer it is necessary to measure ice crystal size distributions in order to determine kinetic parameters for icc crystallization. Although fairly precise data could be obtained by this method, it is tedious and a relatively long time is needed for the experiments.

Temperature response experiments are conducted to determine the kinetics for a batch crystallizer. The information on kinetics can be obtained by measuring only the temperature change caused by the release of latent heat upon ice crystal growth in the batch crystallizer. However it is difficult to analyze crystallization of ice in the batch crystallizer mathematically because the population balance equation with respect to ice crystal size must be solved under unsteady state conditions.

Kane et al. (1974) solved the population balance equation for batch crystallizers on the assumption that the linear growth rate of ice crystals is independent of crystal size, and derived an equation to determine the kinetic parameter β, the nucleation rate per crystal in continuous crystallizers, from the maximum slope of the temperature response curve, where the β is an increasing function of the growth and nucleation rates. However the linear growth rate of ice crystals is not always independent of the size under the experimental conditions examined. For instance, the growth rate might be size-dependent if heat transfer governs the growth process. Thus the objective of the present study is to extend the method proposed by Kane et al. (1974) to a more general method which takes into account the crystal size dependency of the growth rate.

The temperature response curve and the crystal size distribution were observed with a highly sensitive thermistor and a microscope during batch crystallizations of pure water and of a 5% dextran solution. The data obtained were compared with the theoretical data for justification of the method.

CONCLUSIONS AND SIGNIFICANCE

In this paper we solved a population balance equation with respect to crystal size for a batch crystallizer on the assumption that the ice crystal growth rate could be expressed by $Ga = g_{a0} + g_{a-1}/r$, and then obtained a correlation to determine the parameter β. Calculated temperature changes with crystal growth in a batch crystallizer and crystal size distributions of the ice formed were found to be in good agreement with those obtained experimentally on the assumption that the growth rate is limited only by a heat transfer process not only in pure water but also in a polymer solution of 5% dextran.

The method of simulation is easily extended to other experimental conditions in which growth rates are limited by a mass transfer process, intrinsic kinetics, and so on, by using the respective relationships between the growth rate parameters, g_{a0} and g_{a-1}, and the subcooling.

Thus crystal size distribution of ice might be predicted for the case of any mechanism of crystal growth with any known initial subcooling if the maximum slope of the temperature response curve is obtained experimentally.

Correspondence concerning this paper should be addressed to Ryuichi Matsuno.

INTRODUCTION

Freeze concentration is of greater advantage than conventional evaporation methods for liquid foods. The procedure permits avoidance of thermal degradation, decreases loss of aroma during concentration, and possibly saves energy. However, freeze concentration is not in wide use in industrial applications due to lack of information on the kinetics for secondary nucleation and growth of ice crystals in liquid foods which consist of a number of components including high molecular weight substances.

Huige and Thijssen (1972) have studied the kinetics of ice crystallization for a sucrose solution in a mixed suspension, mixed product removal (MSMPR) type crystallizer. Several investigators (Evans et al., 1974a; Omran and King, 1974; Kane et al., 1974; Stocking and King, 1976) have studied the kinetics of ice crystallization by a thermal response method in a batch crystallizer. The method is very convenient for determining the kinetic parameters for the growth rate and secondary nucleation of ice crystals because the kinetics can be estimated by measuring only the temperature change which is caused by the release of latent heat owing to the growth of ice crystals in the crystallizer.

Omran and King (1974) and Stocking and King (1976) obtained kinetic parameters from the initial stage of the temperature response curve on the assumption of an ice crystal size-dependent growth rate. Kane et al. (1974) solved the population balance equation with respect to ice crystal size and calculated a temperature change in a whole course of batch crystallization up to equilibrium. Furthermore, a correlation to determine the kinetic parameter β, the nucleation rate per crystal in continuous crystallizers, from the maximum slope of the temperature response curve was derived. β is an increasing function of the growth and nucleation rates and is an important parameter for designing continuous crystallizers. However the assumption made in the theoretical analysis that the linear growth rate is independent of ice crystal size is not always suitable for the usual conditions encountered in batch crystallizers. For instance the linear growth rate of ice crystals increased as the size decreased below about 0.8 mm (Margolis et al., 1971). Examination of the Sherwood or Nusselt number in the batch crystallization revealed that the linear growth rate of ice crystals is dependent on ice crystal size if the growth rate is assumed to be limited by a heat or mass transfer process.

Thus we propose in the present study a method to calculate the change in temperature and crystal size distribution during the course of batch crystallization, taking into account the crystal size dependency of the growth rate. An equation for estimating the β values from the maximum slope of the temperature change curve is derived, after examination of the validity of the method by comparing calculated results with not only the temperature profile but also the crystal size distribution found experimentally in water and a dextran solution.

THEORY

We would like to consider the situation in which a seed ice crystal is introduced into an adiabatic batch crystallizer kept at a certain degree of subcooling ΔT^o. To follow theoretically the change in the temperature due to the release of latent heat of crystallization and the crystal size distribution, a population balance equation with respect to crystal size and a heat balance equation must be solved simultaneously.

Assumption

1. The ice crystals are of a disc shape having a radius r and height $2z$ and the aspect ratio z/r is independent of crystal size. The latter assumption implies

$$Gc/Ga = z/r = a \tag{1}$$

where Ga and Gc are the linear growth rates of the a and c axes, respectively, and a is a constant (Kane et al., 1974).

2. Ga and Gc are size-dependent as follows,

$$Ga = g_{a0} + g_{a-1}/r \tag{2}$$

$$Gc = g_{c0} + g_{c-1}/r \tag{3}$$

where g_{a0} and g_{c0} are the growth rate constants of the a and c axes for the size-independent terms, and g_{a-1} and g_{c-1} are those for the size-dependent terms. They are functions of subcooling.

3. New crystals are nucleated at near zero size (Kane et al., 1974).

4. The secondary nucleation rate $\dot{N}$ is proportional to the nth moment of particle size distribution, μ_n (Kane et al., 1974).

$$\dot{N} = a_n \mu_n \tag{4}$$

where a_n is constant and a function of subcooling. Here, the nth moment μ_n is defined by using the distribution function f with respect to r as

$$\mu_n = \int_0^\infty f r^n dr \tag{5}$$

Basic Equation

The population balance equation and the heat balance equation are basically the same as those adopted by Kane et al. (1974).

$$\frac{\partial f}{\partial t} + \frac{\partial f Ga}{\partial r} = a_n \mu_n \delta(r - 0) \tag{6}$$

$$\rho Cp \frac{dT}{dt} = \lambda \rho_I \int_0^\infty \frac{dVc}{dt} f dr \tag{7}$$

$$\frac{dVc}{dt} = 6\pi r^2 Gc \tag{8}$$

where $\delta(r - 0)$ is the Dirac delta function, ρ is the density of solution, Cp is the specific heat, T is the temperature, λ is the heat of thawing of ice, ρ_I is the density of ice, and Vc is the volume of an ice particle. Equation 7 is rearranged as Eq. 9 by combining Eqs. 3 and 8.

$$\rho Cp \frac{dT}{dt} = 6\pi \lambda \rho_I (g_{c0}\mu_2 + g_{c-1}\mu_1) \tag{9}$$

The simultaneous differential equations, Eqs. 5, 6, and 9, cannot be solved analytically. However, under the constant subcooling condition for a short time increment, the distribution function f is obtained analytically by solving Eq. 6 and the resultant moments μ_1 and μ_2 are used for the calculation of temperature change from Eq. 9. These procedures are repeated until an equilibrium is reached.

Solution of the Population Balance Equation

The procedure for solving Eq. 6 by the Laplace transformation method is applicable to any value of n, however the complexity of mathematical algebra increases tremendously for higher values of n. Equation 6 was solved only for the case in which the nucleation rate is proportional to the second moment of crystal size μ_2. The analytical solutions for f, μ_0, μ_1, and μ_2 under constant subcooling are obtained with Eqs. A-8 to A-11 in the appendix.

The Basic Parameter β

The kinetic parameter β, the nucleation rate per crystal in a continuous crystallizer, is related to the average residence time τ in the continuous crystallizer as shown in Eq. 10 (Kane et al., 1974).

$$\beta = \frac{a_n \mu_n}{\mu_0} = \frac{a_n \mu_n}{\dot{N}\tau} = \frac{1}{\tau} \tag{10}$$

The relation of β to the growth and nucleation rate parameters of ice crystals is derived. The population balance equation for the continuous crystallizer at steady state is written as

$$\frac{d}{dr}(g_{a0} + g_{a-1}/r)f = -\frac{f}{\tau} \tag{11}$$

Combining the solution of Eq. 11 with Eq. 10, we obtain

$$\int_0^\infty \frac{a_n g_{a0}^n}{\frac{r}{g_{a0}} + \frac{g_{a-1}}{g_{a0}^2}} \left(\frac{r}{g_{a0}}\right)^{n+1} \exp\left[-\beta\left(\frac{r}{g_{a0}} - \frac{g_{a-1}}{g_{a0}^2}\ln\frac{\frac{r}{g_{a0}} + \frac{g_{a-1}}{g_{a0}^2}}{\frac{g_{a-1}}{g_{a0}^2}}\right)\right] d\left(\frac{r}{g_{a0}}\right) = 1 \tag{12}$$

where

$$\frac{g_{a-1}}{g_{a0}^2} = \frac{1}{2}\cdot\frac{\beta_1^{(n+2)/n}}{\beta_2^{2(n+1)/n}}\left[\Gamma\left(\frac{n}{2}+1\right)\right]^{2/n},$$

$$\beta_1 = \left[a_n(2g_{a-1})^{n/2}\Gamma\left(\frac{n}{2}+1\right)\right]^{2/(n+2)}$$

$$\beta_2 = (n!a_n g_{a0}^n)^{1/(n+1)}$$

If n is assumed to be 2, Eq. 12 is rearranged as Eq. 13, and β_1 and β_2 in Eq. 13 correspond to β_1 and β_2 in Eq. A-8.

$$\int_0^\infty \frac{\beta_2^3 y^3/2}{\beta_1^2/\beta_2^3 + y}\exp(-\beta\phi)dy = 1 \tag{13}$$

where

$$\phi = y - \frac{\beta_1^2}{\beta_2^3}\ln\frac{y + \beta_1^2/\beta_2^3}{\beta_1^2/\beta_2^3}, \quad y = \frac{r}{g_{a0}}$$

Equation 13 shows that β is the function of the two parameters β_1 and β_2 defined in Eq. A-8, which contain the growth and nucleation parameters. The relationship among β, β_1, and β_2 is calculated numerically by Eq. 13.

For determination of β from the experimental temperature response curve, a correlation between β and the maximum slope of the temperature response curve $(dT/dt)_{max}$ is useful (Kane et al., 1974). To obtain the correlation, numerous temperature response curves were calculated for various initial subcoolings ΔT^o and second moments μ_2^o under varieties of g_{a0}, g_{a-1} and a_2 values. Finally, the initial β value, β^o was correlated by

$$\Delta T^o\beta^o = 5.93(\mu_2^o)^{0.027}(dT/dt)_{max} \tag{14}$$

Procedure for Simulation of Temperature Response Curve and Particle Size Distribution

In this paper, the growth rate of the a axis was assumed to be limited by a heat transfer process and to be proportional to the subcooling not only in pure water but also in a solution containing a substance of high molecular weight because little freezing point depression was observed in the solution. The growth rate constants are proportional to the subcooling and are shown below:

$$g_{a-1} = A_1\Delta T, \quad g_{c-1} = aA_1\Delta T,$$
$$g_{a0} = A_2\Delta T, \quad g_{c0} = aA_2\Delta T \tag{15}$$

Knowledge of the growth rate constants A_1 and A_2 defined in Eq. 15 is necessary to simulate the temperature response curve and particle size distribution. Since the crystal growth rate was assumed to be limited by a heat transfer process, the values of A_1 and A_2 are estimated from a correlation for the Nusselt number, Nu, proposed by Huige and Thijssen (1972):

$$Nu = 2 + 1.3(\epsilon d^4/\upsilon^3)^{0.17}Pr^{0.25} \tag{16}$$

where ϵ is the average power input, υ the kinematic viscosity, Pr the Prandtl number, and d the particle diameter.

Using the heat transfer coefficient h, the volumetric growth rate is written by

$$\frac{dVc}{dt} = \frac{(2\pi r^2 + 4\pi a r^2)h\Delta T}{\rho_I\lambda} \tag{17}$$

Then a linear growth rate for the a axis is expressed as Eq. 18 by combining Eq. 17 with Eqs. 1 and 8.

$$Ga = \frac{(1 + 2a)h\Delta T}{3a\rho_I\lambda} \tag{18}$$

Comparison of Eq. 18 after substitution of Eq. 16 for h with Eq. 2 yields

$$A_1 = \frac{(1 + 2a)^2 k}{9a^2\rho_I\lambda} \tag{19}$$

$$A_2 = \frac{1.3(1 + 2a)^2 k}{18a^2\rho_I\lambda}\left[\epsilon\left(\frac{6a}{1 + 2a}\right)^4/\upsilon^3\right]^{0.17}Pr^{0.25}/r^{0.32} \tag{20}$$

where k is the thermal conductivity. For the derivation of Eqs. 19 and 20, the equivalent diameter, d_e, defined by Eq. 21 is used for the diameter which appeared in Eq. 16.

$$d_e = \frac{6 \times \text{volume of a particle}}{\text{surface of a particle}} = \frac{6a}{1 + 2a}\cdot r \tag{21}$$

Contrary to the assumption, Eq. 20 shows a slight dependence on r. Then each representative value of A_2, 8.5×10^{-5} and 6.3×10^{-5} m/s·K, was used for water and dextran solution systems, respectively. The value was two-thirds of the value calculated by Eq. 20 using each average maximum radius found in many experiments and the measured power input per unit mass ϵ under experimental condition.

The nucleation rate was assumed to be proportional to the second power of the subcooling as well as to the second moment of crystal size distribution. Stocking and King (1976) showed that the nucleation rate is proportional to the second power of the subcooling in sucrose solutions from their thermal response experiments. The nucleation rate constant, a_2, is:

$$a_2 = A_3\Delta T^2 \tag{22}$$

The procedure for simulation of a temperature response curve is as follows.

1. The initial second moment μ_2^o is assumed.
2. The initial β^o value is calculated from the experimental maximum slope of a temperature response curve using Eq. 14.
3. From β^o, A_1, A_2 and ΔT^o, the A_3 value is determined using Eq. 13.
4. The temperature response curve and the crystal size distribution are calculated using Eqs. 9, A-8, A-9, A-10, and A-11.
5. The calculated result is compared with the experimental result. If a good agreement is not obtained, another μ_2^o is assumed and the procedure is repeated.

EXPERIMENTAL

Apparatus

Figure 1 shows a schematic diagram of the experimental apparatus. The crystallizer used was a cylindrical vessel (56 mm dia. × 125 mm) equipped with a double jacket and made of acryl resin. Refrigerant, an ethylene glycol solution, was circulated between the jacket adjacent to the crystallizer and a coolant tank by a pump (Iwaki MD40R). The other jacket placed outside the crystallizer was filled with air to prevent heat loss. A circular acryl plate 15 mm thick was placed at the top of the crystallizer as a cover. This plate had a small hole for the injection of a seed crystal, and was removed when ice crystals were observed with a traveling microscope (Nikon SMZ-10). The whole crystallizer and the connection tubes were covered with sponge sheets for heat insulation. Two oil seals were set at the center of the bottom of crystallizer and that of the jacket, respectively. The agitator shaft passed through these oil seals and was connected to a motor (75W Tokyo Rikakikai MS-75) placed under the crystallizer. The agitator propeller had four blades and was positioned with its disk plane about 30 mm above the bottom of the crystallizer. The agitation speed was kept constant at 600 rpm in all the experiments. The crystallizer was equipped with four equal acryl baffles of 5 mm width (Figure 1). The temperature of the coolant was controlled

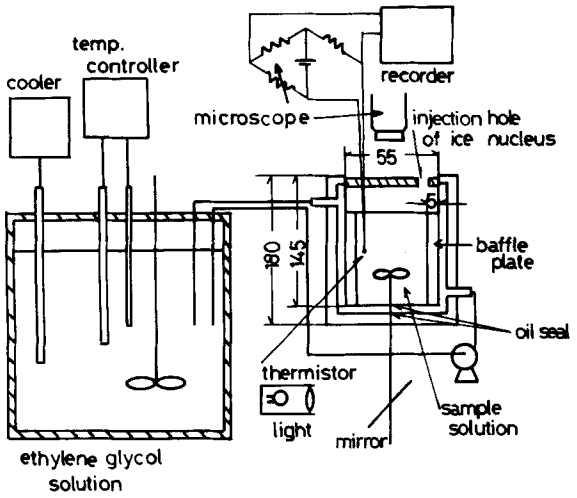

Figure 1. Experimental apparatus.

with a cooler (Neslab Bath Cooler PBC-4) and a thermistor system (Neslab Exatrol), and the temperature of the solution in the crystallizer was kept constant within ± 0.001 K. The temperature of the solution was detected with a thermistor (Ishizuka Denshi 512CT) set 45 mm above the bottom of the crystallizer, and was drawn on a recorder (Rikadenki R-11). The light beam passed through the transparent solution in the crystallizer and reached the microscope set above the top of the crystallizer.

Thermal Response Experiment

The experimental procedure was as follows. A 170 ml sample of solution was allowed to stand in a vacuum for a moment to expel dissolved air, and a part of the solution was frozen in a freezer. The same sample solution was used for six or seven experiments. The temperature of the sample solution was adjusted beforehand to the prescribed degree of subcooling by controlling the temperature of the coolant. The degree of subcooling was varied between 0.03 and 0.2 K. After it was confirmed that the temperature of the solution had been kept constant within ± 0.001 K, a seed ice crystal was introduced to initiate crystallization. A seed ice crystal was prepared as follows: A drop of water, 3 μL, formed at the tip of a needle of a microsyringe (Terumo MS-G 10) was frozen with dry ice. The seed ice crystal formed was rinsed with ice water to smooth the surface and to prevent initial breeding. The seeding was conducted by inserting the needle with the seed crystal through the injection hole and shaking it to make the crystal drop off. The moment the seed crystal dropped into the solution, the recorder was started, and the temperature change of the solution was recorded. Distilled water and 5% Dextran T500 solution (Pharmacia Fine Chemical, m.w. 500,000) were used as sample solutions.

Determination of Ice Crystal Sizes

After the temperature of the sample solution reached equilibrium, the agitation was stopped, the upper cover of the crystallizer was removed, and the ice crystals formed and lifted near the surface of the solution were observed with a traveling microscope at a magnification of 20X. About 200–300 ice crystals were photographed in every experiment.

Values of Physical Properties

The viscosity of 5% Dextran T500 solution at 273 K was determined as 0.0125 kg/m·s by a B-type viscometer (Tokyo Keiki Seisakusho). The physical properties of water at 273 K as given in *Handbook of Chemistry and Physics* (Weast, 1966–1967) are: thermal conductivity k, 0.567 J/m·s·K; density ρ, 1×10^3 kg/m^3; viscosity, 0.0018 kg/m·s. The values of thermal conductivity and density of the dextran solution were assumed to be the same as those of water.

RESULTS

Ice Crystals Formed in Pure Water and Dextran Solution

Figure 2 shows typical photographs of ice crystals formed in pure water and 5% Dextran T500 solution. As assumed, disc-shaped ice

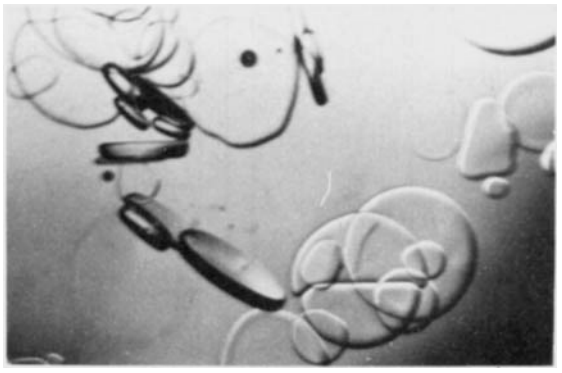

Fig. 2-a. $\Delta T° = 0.056$ K

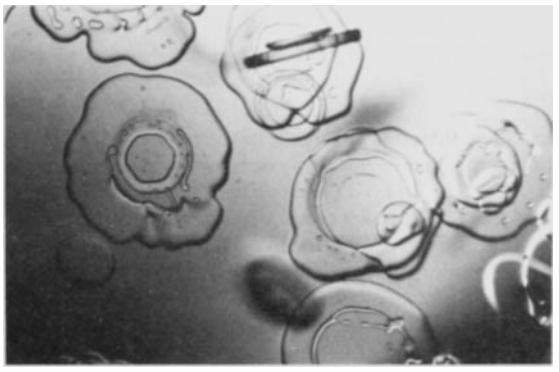

Fig. 2-b. $\Delta T° = 0.055$ K

Figure 2. Microscopic photographs of ice crystals formed in pure water (Figure 2-a) and in 5% Dextran T500 solution (Figure 2-b) at a magnification of twenty.

crystals were observed both in pure water and the dextran solution. The crystals formed in water had a very smooth and transparent surface, while a pattern of radially spreading small grains like bubbles and some ditches in places were observed on the surface of the crystals formed in the dextran solution. The height-to-diameter ratios of the ice crystals were determined by measuring the height and the diameter of the ice crystals floating vertically in the sample solution under a wide range of subcooling. The average ratios of 42 and 80 crystals were 0.141 and 0.131 for pure water and 5% Dextran T500 solution, respectively.

Temperature Response Curve

Examples of the temperature response curves observed are shown in Figure 3. Since the shape of the seed crystal (sphere) was

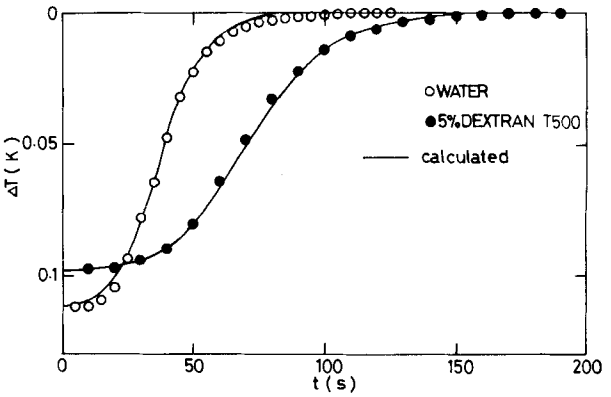

Figure 3. Comparison of predicted and experimental temperature response curves.

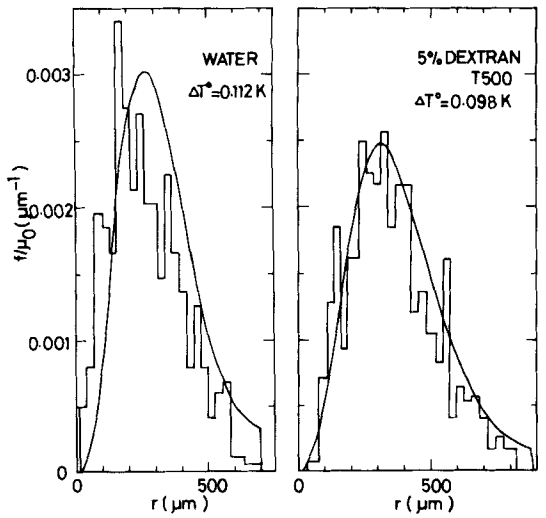

Figure 4. Comparison of predicted and experimental ice crystal size distributions.

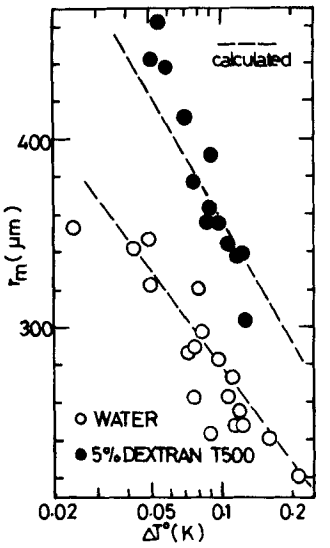

Figure 5. Comparison of predicted and experimental mean sizes of ice crystals with change of initial subcoolings.

completely different from that of the nucleated ones (disc), theoretical temperature response curves were calculated from Eqs. 9, A-8, A-9, A-10, and A-11 under various values of the initial second moment μ_2^0. The smaller the μ_2^0 value, the longer the induction time (Stocking and King, 1976), while the maximum slope of the temperature response curve changed slightly with the change in μ_2^0. Equation 14 also shows the low dependency of the maximum slope on the μ_2^0 value. The proper selection of the μ_2^0 value results in a fairly good agreement in temperature response with the observed one as shown in Figure 3. The best-fit values of μ_2^0 for many experiments corresponded to a one to two times larger radius than the equivalent radius having the same surface area as that of the seed crystal.

Ice Crystal Size Distribution

The changes in crystal size distribution with time both in pure water and 5% Dextran T500 solution were calculated from Eqs. A-8 to A-11 and the final crystal size distribution near equilibrium is compared with experimental one in Figure 4. A fairly good agreement is found between them. The effect of the initial second moment μ_2^0 on the mode of calculated crystal size distribution is insignificant as that on the maximum slope of a temperature response curve. This suggests that final crystal size distribution is predictable with the knowledge of initial subcooling and the maximum slope irrespective of the values of μ_2^0 under the assumption of growth rate being limited by a heat transfer process.

Mean Size of Ice Crystals

The nucleation rate constants A_3 were determined from the maximum slope of various experimental temperature response curves with different initial subcoolings using Eq. 13, and the average value was used for calculation of the change in a final mean crystal size with initial subcooling using Eqs. A-10 and A-11. The calculated results fit with experimental ones as shown in Figure 5.

DISCUSSION

The simulation made under the assumption that the growth rate of ice crystals is limited by a heat transfer process and the nucleation rate is proportional to the second moment of ice crystal size distribution and the second power of the subcooling reproduced well the experimental results both in the temperature response curve and the crystal size distribution. The appropriateness of the assumption on the growth rate of ice crystals under the experimental conditions used is in accord with the studies so far reported (Harriot, 1967; and Margolis et al., 1971). The assumption was applicable even to the 5% Dextran T500 solution. This might be ascribable to the fact that little freezing point depression was observed because of the high molecular weight of dextran.

The method of simulation presented is easily extended to other experimental conditions in which rates are limited, such as by a diffusional process, intrinsic kinetics, and so on, by using the respective relationships between the growth rate parameters, g_{a0}, g_{a-1} and the subcooling.

The dependency of the secondary nucleation rate on subcooling can be determined by the induction time method (Omran and King, 1974; Stocking and King, 1976) irrespective of the order of the moment of crystal size distribution on which the nucleation rate depends. At subcooling between 0.25 and 1.0 K, Omran and King (1974) reported that the nucleation rate depends on slightly higher than first-order subcooling in a batch crystallizer, while Stocking and King (1976) showed that the nucleation rate increases with approximately the second power of subcooling at subcoolings between 0.01 and 0.2 K. We assumed that the nucleation rate is proportional to the second power of the initial subcooling because the degree of subcooling under our experimental conditions is in accord with that of Stocking and King.

There have been many discussions on the mechanism of secondary nucleation (Melia and Moffitt, 1964; Cayey and Estrin, 1967; Clontz and McCabe, 1971; Strickland-Constable, 1972; Ottens et al., 1972; Evans et al., 1974a; Estrin et al., 1975; Toyokura and Hirasawa, 1976). Some attributed the mechanism of secondary nucleation of ice crystals to the fluid shear on the surface of crystals (Estrin et al., 1975), and others to the collision frequency and collision energy (Evans et al., 1974b). These mechanisms imply that the nucleation rate is dependent on the second moment of crystal size distribution or higher moments. Huige (1972) assumed the dependence on nucleation rate on the second moment as in this study. Evans et al. (1974a) showed that the moment can be inferred by changing the coating on the impeller in the crystallizer and indeed derived an order of between two and three.

To fit the theoretical induction time with the experimental time, the initial second moment should have been calculated using a one to two times larger radius than the equivalent radius having the same surface area as that of the seed crystal. Apparent agreement between μ_2^0 and the actual seed character is evidence that very likely the seed dominates the secondary nucleation in the induction part of a batch experiment. This is supported by the induction time dependence and comments of Omran and King (1974).

The β value evaluated for 5% dextran solution was smaller than that for water. This might be due to a decrease in the nucleation rate constant A_3, since A_1 and A_2 might not decrease because of

the high molecular weight of dextran. The decrease in A_3 by addition of a substance of high molecular weight has also been reported by Omran and King (1974).

The existence of the β value for the case of size-dependent growth rate was postulated theoretically by Kane et al. (1974). The concrete relation between β and the rate constants for growth and nucleation was derived in the present study as shown in Eq. 12.

ACKNOWLEDGMENT

The authors gratefully thank Y. Ashida and M. Yamazaki for their help in the experimental work.

NOTATION

a = ratio of growth rates of a and c axes of ice
a_n = nucleation rate constant, Eq. 4, nuclei/s·m^n
A_1 = growth rate constant of a axis of ice, Eq. 19, m^2/s·K
A_2 = growth rate constant of a axis of ice, Eq. 20, m/s·K
A_3 = nucleation rate constant, Eq. 22, nuclei/s·m^2·K^2
d = particle diameter, Eq. 16, m
d_e = equivalent diameter, Eq. 21, m
f = crystal size distribution, m^{-4}
$\bar{f}$ = Laplace transform of f with respect to time, s/m^4
g_{a0} = component of Eq. 2, m/s
g_{a-1} = component of Eq. 2, m^2/s
g_{c0} = component of Eq. 3, m/s
g_{c-1} = component of Eq. 3, m^2/s
Ga = growth rate parallel to basal plane, m/s
Gc = growth rate normal to basal plane, m/s
h = heat transfer coefficient, J/m^2·s·K
k = thermal conductivity, J/m·s·K
n = dependency of actual nucleation rate $\dot{N}$ on crystal size
$\dot{N}$ = actual nucleation rate, Eq. 4, nuclei/s·m^3
Nu = Nusselt number
p = variable in Laplace domain, s^{-1}
Pr = Prandtl number
r = radius of disc crystal, m
r_m = mean radius of disc crystals, m
t = time, s
T = temperature, K
$(dT/dt)_{max}$ = maximum slope of temperature response curve, K/s
ΔT = subcooling, K
Vc = volume of crystal, m^3
z = half height of a disc crystal, m

Greek Letters

β = kinetic parameter, nucleation rate per crystal in continuous crystallizers, Eqs. 12 and 13, s^{-1}
β_1 = β value in the case that growth rate depends on crystal size, s^{-1}
β_2 = β value in the case that growth rate is independent of crystal size, s^{-1}
ϵ = power input per unit mass of sample solution, m^2/s^3
λ = latent heat of fusion, J/kg
ρ = fluid density, kg/m^3
ρ_I = density of ice, kg/m^3
τ = average residence time of crystals in continuous crystallizers, s
μ_n = nth moment of crystal size distribution, m^n/m^3
$\bar{\mu}_n$ = Laplace transform of μ_n with respect to time, m^n·s/m^3
υ = kinematic viscosity, m^2/s

APPENDIX

Laplace transformation of Eq. 6 with respect to time in the case $n = 2$ yields

$$p\bar{f} = -\frac{d}{dr}(g_{a0} + g_{a-1}/r)\bar{f} + a_2\bar{\mu}_2\delta(r \sim 0) + f^o \qquad \text{(A1)}$$

Integration of Eq. A-1 with respect to r gives

$$\bar{f} = \frac{a_2\bar{\mu}_2}{g_{a0} + g_{a-1}/r}\exp\left[-\frac{p}{g_{a0}^2}\left(g_{a0}r - g_{a-1}\ln\frac{g_{a0}r + g_{a-1}}{g_{a-1}}\right)\right] + \frac{1}{g_{a0} + g_{a-1}/r}\int_0^r f^o \exp\left[\frac{p}{g_{a0}^2}\left((\xi - r)g_{a0} + g_{a-1}\ln\frac{g_{a-1} + rg_{a0}}{g_{a-1} + \xi g_{a0}}\right)\right]d\xi \qquad \text{(A2)}$$

The solution of the second moment of crystal size distribution, μ_2, is needed for the inverse Laplace transformation of Eq. A2. Multiplying Eq. 6 by r^m and integrating with respect to r from 0 to ∞ yields

$$\frac{d\mu_m}{dt} = g_{a-1}m\mu_{m-2} + g_{a0}m\mu_{m-1} + \delta_{0m}a_2\mu_2 \qquad \text{(A3)}$$

where δ_{0m} is the Kronecker delta. Equation A3 is transformed to the Laplace domain and the following sets of arithmetic equations are obtained:

$$p\bar{\mu}_0 - \mu_0^o = a_2\bar{\mu}_2 \qquad \text{(A4)}$$

$$p\bar{\mu}_1 - \mu_1^o = g_{a-1}\bar{\mu}_{-1} + g_{a0}\bar{\mu}_0 \qquad \text{(A5)}$$

$$p\bar{\mu}_2 - \mu_2^o = 2g_{a-1}\bar{\mu}_0 + 2g_{a0}\bar{\mu}_1 \qquad \text{(A6)}$$

where μ_n^o is the initial value of the nth moment. Since these three sets of equations contain four unknown moments, μ_0, μ_1, μ_2 and μ_{-1}, $\bar{\mu}_2$ cannot be derived. Among these moments, the change in μ_{-1} with time is the smallest except near zero time. So the μ_{-1} is assumed to be constant for a short time interval. Then, Eq. A5 is rewritten as Eq. A5′.

$$p\bar{\mu}_1 - \mu_1^o = g_{a-1}\mu_{-1}/p + g_{a0}\bar{\mu}_0 \qquad \text{(A5′)}$$

From Eqs. A4, A5′ and A6, $\bar{\mu}_2$ is solved as

$$\bar{\mu}_2 = \frac{2\mu_0^o(g_{a-1}p + g_{a0}^2) + 2g_{a0}(g_{a-1}\mu_{-1} + p\mu_1^o) + p^2\mu_2^o}{p^3 - \beta_1^2 p - \beta_2^3} \qquad \text{(A7)}$$

The inverse Laplace transformation of Eq. A7 gives Eq. A9. In the same way, μ_0 and μ_1 are obtained by Eqs. A10 and A11. After substitution of Eq. A7, Eq. A2 is subjected to inverse Laplace transformation and Eq. A8 is obtained:

$$\left.\begin{aligned} f &= \frac{r}{g_{a-1} + rg_{a0}}\left[Ae^{\alpha\Delta t} + e^{-1/2\alpha\Delta t}\left(B_1\cos\frac{\sqrt{3}}{2}\gamma\Delta t - B_2\sin\frac{\sqrt{3}}{2}\gamma\Delta t\right)\right] \\ &\text{for } \Delta t = t - \left(rg_{a0} - g_{a-1}\ln\frac{g_{a-1} + rg_{a0}}{g_{a-1}}\right)\Big/ g_{a0}^2 \geqq 0 \\ f &= \frac{g_{a-1} + g_{a0}\xi}{\xi}\cdot\frac{r}{g_{a-1} + rg_{a0}}f^o(\xi) \\ &\text{for } \Delta t < 0 \end{aligned}\right\} \qquad \text{(A8)}$$

where ξ is a root of

$$\ln\left(1+\frac{(\xi-r)g_{a0}}{g_{a-1}+rg_{a0}}\right)=\frac{g_{a0}}{g_{a-1}}(\xi-r)+\frac{g_{a0}^2}{g_{a-1}}t$$

$$A=\frac{a_2\mu_2^o\alpha^2+s\alpha+L}{3\alpha^2-\beta_1^2},$$

$$B_1=\frac{2M(a_2\mu_2^oQ-s\alpha/2+L)+9\alpha\gamma^2(a_2\mu_2^o\alpha-s)/2}{M^2+27\alpha^2\gamma^2/4},$$

$$B_2=\frac{3\sqrt{3}(a_2\mu_2^oQ-s\alpha/2+L)\alpha\gamma-\sqrt{3}M\gamma(a_2\mu_2^o\alpha-s)}{M^2+27\alpha^2\gamma^2/4},$$

$$s=\frac{\beta_2^3\mu_1^o}{g_{a0}}+\beta_1^2\mu_0^o,$$

$$L=\beta_2^3\mu_0^o+\beta_1^2g_{a0}\mu_{-1},\quad M=3Q-\beta_1^2,\quad Q=\frac{1}{2}\alpha^2-\frac{3}{4}\gamma^2,$$

$$\beta_1=\sqrt{2a_2g_{a-1}},\quad \beta_2=\sqrt[3]{2a_2g_{a0}^2},$$

$$X=\sqrt[3]{\beta_2^3/2+\sqrt{\beta_2^6/4-\beta_1^6/27}},$$

$$Y=\sqrt[3]{\beta_2^3/2-\sqrt{\beta_2^6/4-\beta_1^6/27}},$$

$$\alpha=X+Y,\quad \gamma=X-Y$$

$$\mu_2=(1/a_2)\left[Ae^{\alpha t}+e^{-1/2\alpha t}\left(B_1\cos\frac{\sqrt{3}}{2}\gamma t-B_2\sin\frac{\sqrt{3}}{2}\gamma t\right)\right] \tag{A9}$$

$$\mu_0=\frac{A}{\alpha}e^{\alpha t}+B_1P_1-B_2P_2+C_1 \tag{A10}$$

$$\mu_1=\frac{Ag_{a0}}{\alpha^2}e^{\alpha t}+B_1P_3g_{a0}+B_2P_4g_{a0}+C_1g_{a0}t+g_{a-1}\mu_{-1}t+C_2 \tag{A11}$$

where

$$P_1=\left(\frac{2\sqrt{3}}{\alpha^2}\gamma e^{-1/2\alpha t}\sin\frac{\sqrt{3}}{2}\gamma t-\frac{2}{\alpha}e^{-1/2\alpha t}\cos\frac{\sqrt{3}}{2}\gamma t\right)\Big/\left(1+\frac{3\gamma^2}{\alpha^2}\right),$$

$$P_2=-\left(\frac{2\sqrt{3}}{\alpha^2}\gamma e^{-1/2\alpha t}\cos\frac{\sqrt{3}}{2}\gamma t+\frac{2}{\alpha}e^{-1/2\alpha t}\sin\frac{\sqrt{3}}{2}\gamma t\right)\Big/\left(1+\frac{3\gamma^2}{\alpha^2}\right),$$

$$P_3=\left(\frac{2\sqrt{3}}{\alpha^2}\gamma P_2-\frac{2}{\alpha}P_1\right)\Big/\left(1+\frac{3\gamma^2}{\alpha^2}\right),$$

$$P_4=-\left(\frac{2\sqrt{3}}{\alpha^2}\gamma P_1+\frac{2}{\alpha}P_2\right)\Big/\left(1+\frac{3\gamma^2}{\alpha^2}\right),$$

$$C_1=\mu_0^o-B_1P_1^o+B_2P_2^o-\frac{A}{\alpha},$$

$$C_2=\mu_1^o-\frac{Ag_{a0}}{\alpha^2}-B_1g_{a0}P_3^o+B_2g_{a0}P_4^o$$

In these equations, the superscript ^{o}denotes the initial values of short time increment. The moment μ_{-1} is numerically calculated by substituting Eq. A8 into Eq. 5.

LITERATURE CITED

Cayey, N. W., and J. Estrin, "Secondary Nucleation in Agitated Magnesium Sulfate Solutions," *Ind. Eng. Chem. Fund.*, **6**, 13 (1967).

Clontz, N. A., and W. L. McCabe, "Contact Nucleation of Magnesium Sulfate Heptahydrate," *Chem. Eng. Prog. Symp. Ser.*, No. 110, **67**, 6 (1971).

Estrin, J., W. L. Wang, and G. R. Youngquist, "Secondary Nucleation Due to Fluid Forces Upon a Polycrystalline Mass of Ice," *AIChE J.*, **21**, 392 (1975).

Evans, T. W., G. Margolis, and A. F. Sarofim, "Mechanisms of Secondary Nucleation in Agitated Crystallizers," *AIChE J.*, **20**, 950 (1974a).

Evans, T. W., A. F. Sarofim, and G. Margolis, "Models of Secondary Nucleation Attributable to Crystal-Crystallizer and Crystal-Crystal Collisions," *AIChE J.*, **20**, 959 (1974b).

Harriot, P., "The Growth of Ice Crystals in a Stirred Tank," *AIChE J.*, **13**, 755 (1967).

Huige, N. J. J., "Nucleation and Growth of Ice Crystals from Water and Sugar Solutions in Continuous Stirred Tank Crystallizers," Ph.D. Dissertation, Univ. Eindhoven, The Netherlands (1972).

Huige, N. J. J., and H. A. C. Thijssen, "Production of Large Crystals by Continuous Ripening in a Stirred Tank," *J. Crystal Growth*, **13/14**, 483 (1972).

Kane, S. G., et al., "Determination of the Kinetics of Secondary Nucleation in Batch Crystallizers," *AIChE J.*, **20**, 855 (1974).

Margolis, G., et al., "The Performance of a Continuous Well-Stirred Ice Crystallizer," *Ind. Eng. Chem. Fund.*, **10**, 439 (1971).

Melia, T. P., and W. P. Moffitt, "Secondary Nucleation from Aqueous Solutions," *Ind. Eng. Chem. Fund.*, **3**, 313 (1964).

Omran, A. M., and C. J. King, "Kinetics of Ice Crystallization in Sugar Solutions and Fruit Juices," *AIChE J.*, **20**, 795 (1974).

Ottens, E. P. K., A. H. Janse, and E. J. De Jong, "Secondary Nucleation in a Stirred Vessel Cooling Crystallizer," *J. Crystal Growth*, **13/14**, 500 (1972).

Strickland-Constable, R. F., "Breeding of Crystal Nuclei: Review of the Subject," *Chem. Eng. Prog. Symp. Ser.*, No. 121, **68**, 1 (1972).

Stocking, J. H., and C. J. King, "Secondary Nucleation of Ice in Sugar Solutions and Fruit Juices," *AIChE J.*, **22**, 131 (1976).

Toyokura, K., and I. Hirasawa, "Shōseki Sōsa to Kakuka-Genshō," *Kagaku Kōgaku*, **40**, 463 (1976).

Weast, R. C., *Handbook of Chemistry and Physics*, 47th ed., the Chemical Rubber Co., Cleveland (1966–1967).

Manuscript received July 7, 1983; revision received Nov. 23, and accepted Dec. 5.